MULTIDISCIPLINARY SCIENCE JOURNAL

RESEARCH ARTICLE
Published Online: November 18, 2024
https://doi.org/10.31893/multiscience.2025269

Reducing aerosol formation from SLS PA12 powder using response surface methodology via optimization of refresh rate and powder handling activities

Amir Abdullah Muhamad Damanhuri[a] | Azian Hariri[b] | Sharin Ab Ghani[c] | Muhammad Hafidz Fazli Md Fauadi[d] | Mohd Syafiq Syazwan Mustafa[e] | Anies Faziehan Zakaria[f] | Ummu Sakinah Subri[g]

[a]Faculty of Mechanical Technology and Engineering, Universiti Teknikal Malaysia Melaka (UTeM), Melaka, Malaysia.
[b]Faculty of Mechanical and Manufacturing Engineering, Universiti Tun Hussein Onn Malaysia, Johor, Malaysia.
[c]Faculty of Electrical Technology and Engineering, Universiti Teknikal Malaysia Melaka (UTeM), Melaka, Malaysia.
[d]Faculty of Industrial and Manufacturing Technology and Engineering, Universiti Teknikal Malaysia Melaka (UTeM), Melaka, Malaysia.
[e]Faculty of Engineering Technology, Universiti Tun Hussein Onn Malaysia, Johor, Malaysia.
[f]Faculty of Engineering and Built Environment, Universiti Kebangsaan Malaysia, Bangi, Malaysia.
[g]Pusat Pengajian Ilmu Pendidikan, Universiti Sains Malaysia, Pulau Pinang, Malaysia.

Abstract A critical issue with Selective laser sintering (SLS) is the release of airborne particulates during powder handling, which pose health risks and environmental concerns. Three factors (input variables) were optimized to minimize the following response variables: particulate matter (PM2.5, PM10), ultrafine particles (UFP), and total suspended particles (TSP) using response surface methodology (RSM). The following parameters were found to minimize the PM2.5, PM10, UFP, and TSP during the pre-processing activities of SLS: (1) Factor A: 100% (100% recycled powder), (2) Factor B: 33% (the powder is thirty-three percent cover when it is collected from the mixing machine), and (3) Factor C: full cover (the powder is completely covered when it is transferred to the SLS 3D printer). These optimal settings resulted in the highest desirability of 0.816. Experiments were conducted using the aforementioned settings to validate the results and the percentage difference between the predicted and experimental values was less than 5%, indicating the reliability of the PM2.5, PM10, UFP, and TSP response surface models. These models will be useful to the operators of SLS 3D printing to predict the PM2.5, PM10, UFP, and TSP as a function of the refresh rate and pre-processing activities considered in this study.

Keywords: additive manufacturing, occupational exposure, particulate matter

1. Introduction

Additive Manufacturing (AM) technologies (otherwise known as three-dimensional (3D) printing), have revolutionized the manufacturing industry. It has been estimated that AM can generate a global economic impact of 200 billion to 600 billion annually by 2025 (Eyers and Potter, 2017). AM technologies have been used to fabricate not only models and prototypes, but also end products. AM technologies have also been used in other sectors such as automotive, aerospace, biomedicine, energy, and consumer goods (Dimov et al., 2001; Ford and Despeisse, 2016; Wong and Hernandez, 2012). In an AM process, an object or prototype is built by joining materials layer by layer. The computer aided design model, which is in stl. format, is optimized first before the model is fabricated using AM technology. According to the American Society for Testing and Materials (now known as ASTM International), AM technologies can be classified into seven categories: (1) material extrusion, (2) material jetting, (3) binder jetting, (4) directed energy deposition, (5) sheet lamination, (6) vat photopolymerization, and (7) powder bed fusion (Huang et al., 2015).

One of the powder bed fusion technologies is Selective Laser Sintering (SLS), which can create complex designs and build many parts simultaneously, depending on the chamber size (Butler, 2011). SLS uses powder feedstock to build prototypes. Carbon dioxide (CO^2) laser beam is used to sinter the powder in a chamber, which is then heated to the melting point of the powder material. A high-powered laser then sinters and binds the powder layer by layer. This process is repeated until the product is completely fabricated. SLS uses various materials such as plastics, nylon, metal, polymers, and ceramics. The powder used for the process can be recycled and reused for the next printing cycle (Prakash et al., 2018), which reduces the overall cost of building the part.

 Received: June 25, 2024 | Accepted: September 04, 2024

While AM offers considerable benefits to the industrial sector, recent reports have noted concerns regarding the potential effects of the process and practices of AM (Rejeski et al., 2018). The use of a three-dimensional (3D) printer in private homes, offices, laboratories, and factories has led to concerns on the emissions of hazardous particles. Short et al. (2015) found that most of the rapid prototyping and AM manufacturers lack health and safety guidelines for users and operators. The operators of AM, particularly SLS 3D printing, are exposed to occupational risks such as air pollutants, and such unconducive working environment can lead to safety and health issues among the workers.

Several researchers have discussed the health hazards of AM operations. Chan et al. (2018) found that among the 46 workers serving various types of AM technology, those involved with 3D printing and AM operations were significantly inflicted with respiratory symptoms. House et al. (2017) noted that the workers use salbutamol inhaler after developing respiratory problems such as asthma following the use of a 3D printer in a small workspace. Ljunggren et al. (2019) conducted biomonitoring and urine test for AM operators dealing with metal powder. They observed the presence of higher metal content in the operators' urine compared to those involved in the office work.

SLS powder contains respirable and inhalable particulates of different sizes, some of which with a diameter of less than 2.5 µm. These particulates are hazardous to both users and operators of SLS 3D printing. Bours et al. (2017) found that the particulate matter (PM) released from handling the powders used for SLS 3D printing increases the risk of physical hazards. Therefore, process control, personal protective equipment, or the use of safer materials may reduce the risks resulting from powder handling.

The key benefits of powder bed fusion technologies are their fine resolution and excellent print efficiency, which makes these technologies ideal for printing complex structures (Ngo et al., 2018). Polymers were the first engineering materials introduced in SLS 3D printing because they can be easily processed (by melting) and they have excellent mechanical properties. At present, the most employed SLS 3D printing materials are semi-crystalline polyamide 12 (PA12) or nylon 12 powders. The PA12 powder dominates the SLS 3D printing market because of its ease-of-use and flexibility in the processing cycle (Dadbakhsh et al., 2017; Tiwari et al., 2015).

The use of virgin powder can increase operating and manufacturing costs. The ratio of virgin powder to the recycled material is known as the refresh rate, and some materials can be used in recycled powder form compared with others. For some materials, the amount of recycled powder affects the strength of the part and the quality of the surface finish (Butler, 2011). Zarringhalam et al. (2006) examined the microstructure and properties of nylon 12 for three types of powder: (1) virgin powder, (2) recycled powder, and (3) refresh rate (67% recycled powder + 33% virgin powder). Dadbakhsh et al. (2016) found that powder aging increased the viscosity and molecular weight of the material. Therefore, the crystallinity of the powder may decrease for aged/recycled powders.

Operators and manufacturers usually mix virgin and recycled powders during SLS 3D printing. In SLS 3D printing, only 20% of the powder is sintered to become the end products in a single processing cycle. Using recycled powders in the next processing cycle is the standard practice of SLS 3D printing, following the recommendations of the suppliers and manufacturers of the powders. SLS 3D printing process involves several processes, most of which involve powder handling such as weighing, mixing, transferring, and pouring the powders. The operators of SLS 3D printing are exposed to the minute particles of the powder because powder handling is done manually and this leads to poor indoor air quality (Ansart et al., 2011; Copelli et al., 2019). Therefore, it is necessary to identify the optimal settings of the refresh rate and powder handling practices to improve the indoor air quality and ensure a safe workplace for the operators involved in SLS 3D printing.

In another research, Mohajer et al. (2015), the levels of total volatile organic compounds (TVOCs) and particulate matter (PM) were tracked in real-time at three different points in time: before, during, and after printing. The results show that the build chamber's built-up aerosols were discharged throughout the printing process when the top cover was opened, producing the highest emission rate during the entire operation.

Even though the post-processing activities of PBF were studied by several researchers (Arrizubieta et al., 2020; Du Preez et al., 2018b; Väisänen et al., 2018), there is a paucity of studies pertaining to the effects of powder bed fusion pre-processing activities on dust exposure. Damanhuri et al. (2019) conducted a pilot study by comparing dust exposure during pre-processing and post-processing activities of a powder bed fusion technology. They found that the following pre-processing activities contribute to large amounts of dust: (1) weighing the powder, (2) collecting the powder from the mixing machine, and (3) transferring the powder into the feeder chamber. It is concluded that the workers can be exposed to the particles during the pre-processing activities.

The novelty of this study lies in the optimization of the pre-processing activities in SLS 3D printing in order to minimize the dust exposure from which the detrimental aerosol originates. The pre-processing activities comprise the refresh rate, collecting the powder from the mixing machine, and transferring of the powder to the feeder chamber of the SLS 3D printer. In this study, the dust exposure is quantified in terms of the particulate matter with a size of less than 2.5 µm (PM2.5), particulate matter with a size of 10 µm (PM10), ultrafine particles (UFP), and total suspended particles (TSP). It is believed that the findings obtained in this study will shed some light on how specific pre-processing activities during SLS 3D printing will affect the aforementioned parameters as well as the optimal pre-processing activity settings that will minimize the dust exposure.

2. Experimental Design

2.1. Morphology of the virgin and recycled PA12 powders

In this study, polyamide nylon PA12 was chosen as the powder for SLS 3D printing. The PA12 virgin powder (bulk density: 0.4 g/cm3, part density: 0.95 g/cm3, melting point: 183 °C, color: white, price: MYR 400/kg) (Farsoon Technologies, 2018) was purchased from local supplier. Before the experiments, the virgin and recycled PA12 powders were characterized by scanning electron microscopy (SEM) and particle size analysis (PSA) (Dadbakhsh et al., 2016; Damanhuri et al., 2019). A scanning electron microscope (Model: TM 3000, Hitachi, Japan) with a magnification range of 5,000–500,000× and operating voltage range of 2.0–5.0 kV was used for this purpose. A particle size analyzer (Zetasizer Nano ZSP, Malvern, UK) was used to determine the particle size distributions of the virgin and recycled PA12 powders. For this analysis, both types of powders were collected, and the particle size distributions were measured before the SLS 3D printing process.

2.2. Layout of experiemental chamber

The pre-processing activities of the SLS 3D printing process were conducted at the SLS Laboratory, Universiti Teknikal Malaysia Melaka (UTeM). The SLS Laboratory (Figure 1) has two 24-m^2 rooms partitioned by a wall. The following pre-processing activities (pouring powder into the mixing machine and transferring the powder to the SLS 3D printer) were performed in Room 2, whereas the following pre-processing activity (pouring powder into the feeder chamber) was performed in Room 1. Both rooms were equipped with a split air conditioner. Each room has an indoor air-conditioning unit and both units are connected to an outdoor unit. The methods for measuring the indoor air concentrations (i.e., sampling point, sample position, sampling period, and sampling technique) were carried out according to the Industry Code of Practice on Indoor Air Quality 2010 (DOSH Malaysia, 2010). The temperature and relative humidity of the laboratory were set at 20 °C and 60%, respectively, to ensure the appropriate working conditions for the SLS 3D printing process. DustTrak DRX aerosol monitor (Model: 8533, TSI Inc., USA) was used to measure the particulate matter concentrations. Two levels were considered for the particulate matter (PM2.5 and PM10), which indicate particulate matter with a diameter of less than 2.5 and 10.0 µm, respectively. P-Trak ultrafine particle counter (Model: 8525, TSI Inc., USA) was used to measure the UFP concentration (Preez et al., 2018; Zontek et al., 2017).

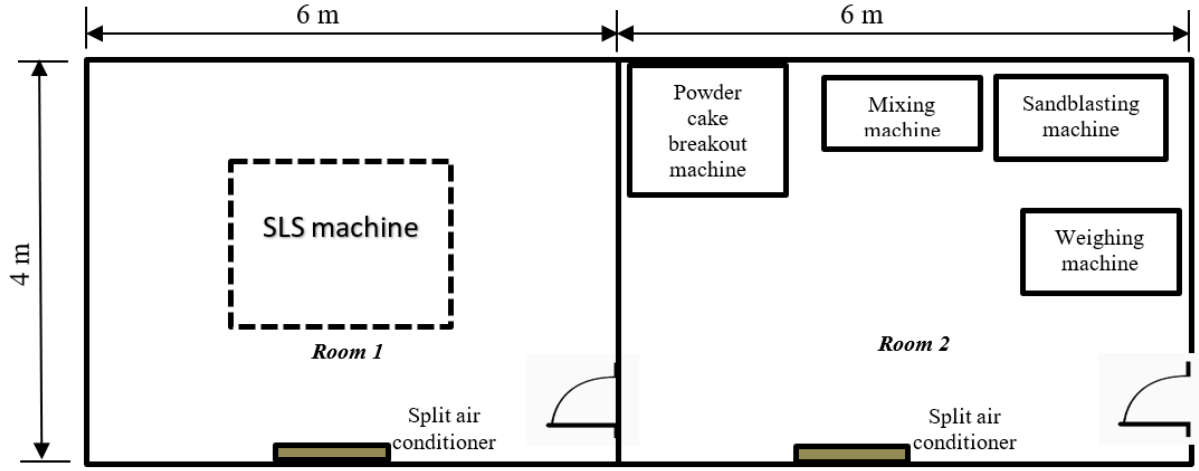

Figure 1 Layout of the SLS 3D printing process workplace.

2.3. Sampling procedure

The exposure to airborne PA12 dust was investigated in this study, where the amount of PA12 powder for SLS 3D printing was fixed at 30 kg. The distance from the fixed datum (floor) to the point where the PA12 powder was poured (pouring height) was fixed at 0.25 m (Plinke et al., 1995). Three factors (Factors A, B, and C), where each factor represents a specific pre-processing activity for SLS 3D printing, as summarized in Table 1. The factors are also the input variables Factor A is the refresh rate, which refers to the mixed powder (i.e., virgin powder + recycled powder). The value for the refresh rate was set from 0% (100% virgin powder) to 100% (100% recycled powder) for the experimental design. Factor B is the pre-processing activity of collecting the powder from the mixing machine, where the value was set as 0% (no cover), 50% (half cover), and 100% (full cover). Factor C is the pre-processing activity of transferring the powder to the feeder chamber of the SLS 3D printer. Factor C is a categorical variable and therefore, the input values are “full cover” and “no cover”, indicating that the activity is carried out completely covered and completely open, respectively (Koponen et al., 2015; Wypych et al., 2005), as shown in Figure 2 (a) and (b).

Table 1 Factors and corresponding values for the experimental design.

Factor (Input variable)	Value	Variable type
A: Refresh rate	0, 50, and 100 (%)	Numeric variable
B: Collecting the powder from the mixing machine	0, 50, and 100%	Numeric variable
C: Transferring the powder to the SLS 3D printer	Full cover and no cover	Categorical variable

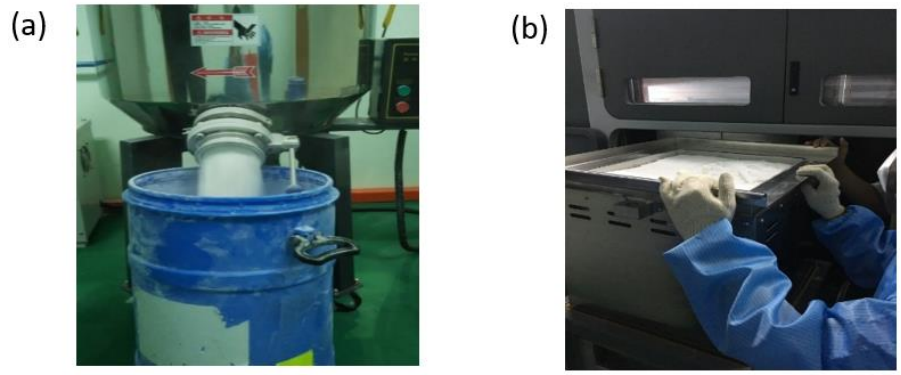

Figure 2 Pre-processing activities for SLS 3D printing considered in this study: (a) collecting powder from the mixing machine and (b) transferring the powder to the feeder chamber.

Design Expert software Version 11.0 (Stat-Ease, Inc., USA) was used to design the experiment based on the central composite design (CCD), which is one of the experimental designs in RSM. Here, the main objective of RSM is to optimize the input variables (Factors A, B, and C) in order to minimize the response variables (PM2.5, PM10, UFP, and TSP) during the pre-processing activities of SLS 3D printing. The input variables are denoted by $X_1, X_2,\ldots, X_k$, where k represents the number of input variables. The response variable is denoted by y. The low-order polynomial model (response surface model) is given by:

$$y = f'(X)\beta + \varepsilon \qquad (1)$$

where $X=(X_1,X_2,\ldots,X_k)'$ and $f(X)$ is the vector function of p elements that consists of the power of $X_1,X_2,\ldots,X_k$ up to a certain degree referred by d, where $d\geq 1$. Referring to Equation (1), the first-order and second-order polynomials (where d=1 and d=2, respectively) can be written as:

$$y = \beta_0 + \sum_{i=1}^{k} \beta_i X_i + \varepsilon \qquad (2)$$

$$y = \beta_0 + \sum_{i=1}^{K} \beta_i x_i + \sum \sum_{i<j} \beta_{ij} \chi_i \chi_j + \sum_{i=1}^{k} \beta_{ii} \chi_i^2 + \varepsilon \qquad (3)$$

where y is the response variable predicted by the response surface model, i is the linear coefficient, j is the quadratic coefficient, β is the regression coefficient, k is the number of input variables (factors), and ε is the random experimental error, which is assumed to have a zero mean. Analysis of variance (ANOVA) was performed on the experimental data to identify the significance of each input variable and response variable. The goodness of fit of the response surface model was assessed based on the coefficient of determination (R^2) and Fisher *F-test* was performed to compare two variances, as indicated by the F-value. The significance of the response surface model was evaluated based on the p-value) for 95% confidence level (Bezerra et al., 2008; Montgomery, 2017). The experimental design matrix is shown in Table 2. The experiment was repeated three times and the average value was determined for the response variables (PM2.5, PM 10, UFP, and TSP).

3. Results and discussion

3.1. Experimental results

Figure 3 (a) and (b) show the morphology of the virgin and recycled powders, respectively. The images were taken at a magnification of 500×. It can be observed that the particles in both types of powders are uniform spheres. According to Chen et al. (2018), spherical particles are conducive for powder flowability because they facilitate the spreading of the powder in the powder bed of the SLS 3D printer. Significant cracks are present in the recycled PA12 powder, which is indeed expected because the powder is previously sintered at a high temperature (200–220 °C). The findings correspond to the results of Dadbakhsh et al. (2017). The origin of the cracks is likely due to the moisture absorbed from the environment during the sintering process and storage (Dotchev and Yusoff, 2009).

Figure 4 shows the particle size distributions of the virgin and recycled PA12 powders obtained from the particle size analyzer. Most of the particles for the virgin and recycled powders are within a size range of 40–60 µm. However, the recycled powder has a higher volume density of particles at a particle size of 60 µm (13%) compared with the virgin powder. The virgin powder has a more uniform size distribution and the highest volume density at a particle size of 50 µm (~10%). This finding conforms with the results Dadbakhsh et al. (2016), who found that there were no significant differences in the size and shape

between the virgin and recycled PA12 powders. Based on their size distributions, the particles from both the virgin and recycled PA12 powders are inhalable and respirable, making them hazardous to the operators' health during powder handling (Kellens et al., 2014).

Table 2 Experimental design matrix.

Experimental run	Input variable			Response variable			
	Factor A: Refresh rate (%)	Factor B: Collecting the powder from the mixing machine (%)	Factor C: Transferring the powder to the SLS 3D printer (full cover or no cover)	PM 2.5 (mg/m³)	PM 10 (mg/m³)	UFP (pt/cc)	TSP (mg/m³)
1	50	50	Full cover	0.401	0.419	5317	0.409
2	0	0	No cover	0.920	0.740	6256	0.342
3	50	0	Full cover	0.592	0.699	5561	0.351
4	50	50	Full cover	0.413	0.445	5377	0.397
5	0	100	No cover	0.834	0.829	5840	0.360
6	0	50	Full cover	0.553	0.412	5669	0.373
7	100	100	No cover	0.416	0.468	5777	0.378
8	50	100	No cover	0.629	0.714	5797	0.392
9	50	50	No cover	0.465	0.542	5588	0.419
10	50	50	No cover	0.453	0.396	5479	0.424
11	100	50	No cover	0.273	0.447	5399	0.424
12	0	100	Full cover	0.838	0.721	5803	0.383
13	50	100	Full cover	0.682	0.676	5582	0.389
14	100	100	Full cover	0.518	0.354	5126	0.355
15	50	50	Full cover	0.409	0.385	5350	0.408
16	0	0	Full cover	0.729	0.638	5792	0.338
17	50	0	No cover	0.716	0.771	5791	0.376
18	100	50	Full cover	0.275	0.336	4942	0.390
19	100	0	Full cover	0.443	0.565	5021	0.359
20	100	0	No cover	0.527	0.658	5398	0.386
21	50	50	No cover	0.465	0.554	5514	0.393
22	0	50	No cover	0.654	0.639	5860	0.394

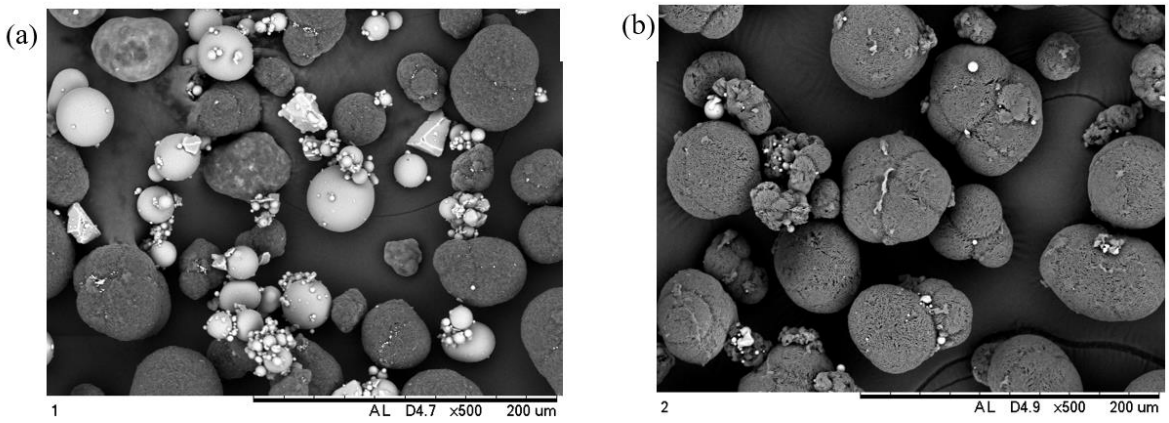

Figure 3 SEM image of the (a) virgin PA12 powder and (b) recycled PA12 powder (magnification: 500×).

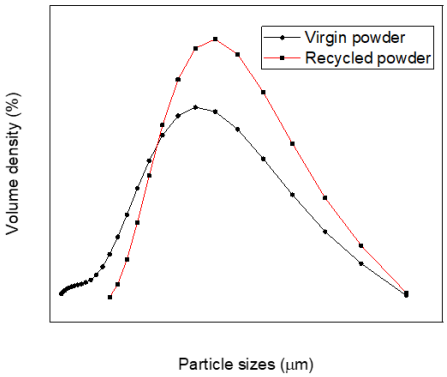

Figure 4 Particle size distribution of the virgin and recycled PA12 powders.

3.2. Analysis of the PM2.5, PM10, UFP and TSP response surface models.

ANOVA was used to assess the significance of the response surface models and the results are presented in Table 3. The experimental data were analyzed, and the response surface model with a *p*-value of less than 0.05 was rated as significant. A *p*-value of less than 0.05 indicates that the variables have a meaningful influence at 95% confidence level. It can be seen from Table 3 that all of the response surface models for PM2.5, PM10, UFP, and TSP have a *p*-value of less than 0.0001, indicating that the models are all significant. In general, a high R^2 value (close to 1) is considered desirable while a fair adjusted R^2 is necessary. The R^2 value indicates that there is good agreement between the experimental data and data predicted by the response surface model (Abdalla et al., 2019). The quadratic model ideally fit to all results based on the R^2 and p value recommended in the DoE software for the predictions of a linear model. It can be seen that the adequate precision *(AP)* is more than 4 for all response surface models, indicating that the models can be used to maneuver the design space. The ANOVA results indicate that all of the response surface models have a positive result (Yusri et al., 2017). Figure 5 (a)–(d) show the normal probability plots of residual for each response surface model. In general, most of the residuals fall within proximity of the straight line, indicating that the PM2.5, PM10, UFP, and TSP response surface models fulfill the normality assumption of a regression model.

Table 3 ANOVA results for the PM2.5, PM10, UFP, and TSP response surface models.

Response surface model	PM2.5[a]	PM10[b]	UFP[c]	TSP[d]
p-value	< 0.0001	< 0.0001	< 0.0001	< 0.0001
F-value	1445.06	24.14	101.24	14.97
R^2	0.9986	0.9062	0.9893	0.9021
Adjusted R^2	0.9979	0.8686	0.9795	0.8418
Adequate precision	134.14	17.68	43.56	13.09

[a]Particulate matter with a diameter of less than 2.5 µm.
[b]Particulate matter with a diameter of less than 10 µm.
[c]Ultrafine particles.
[d]Total suspended particles.

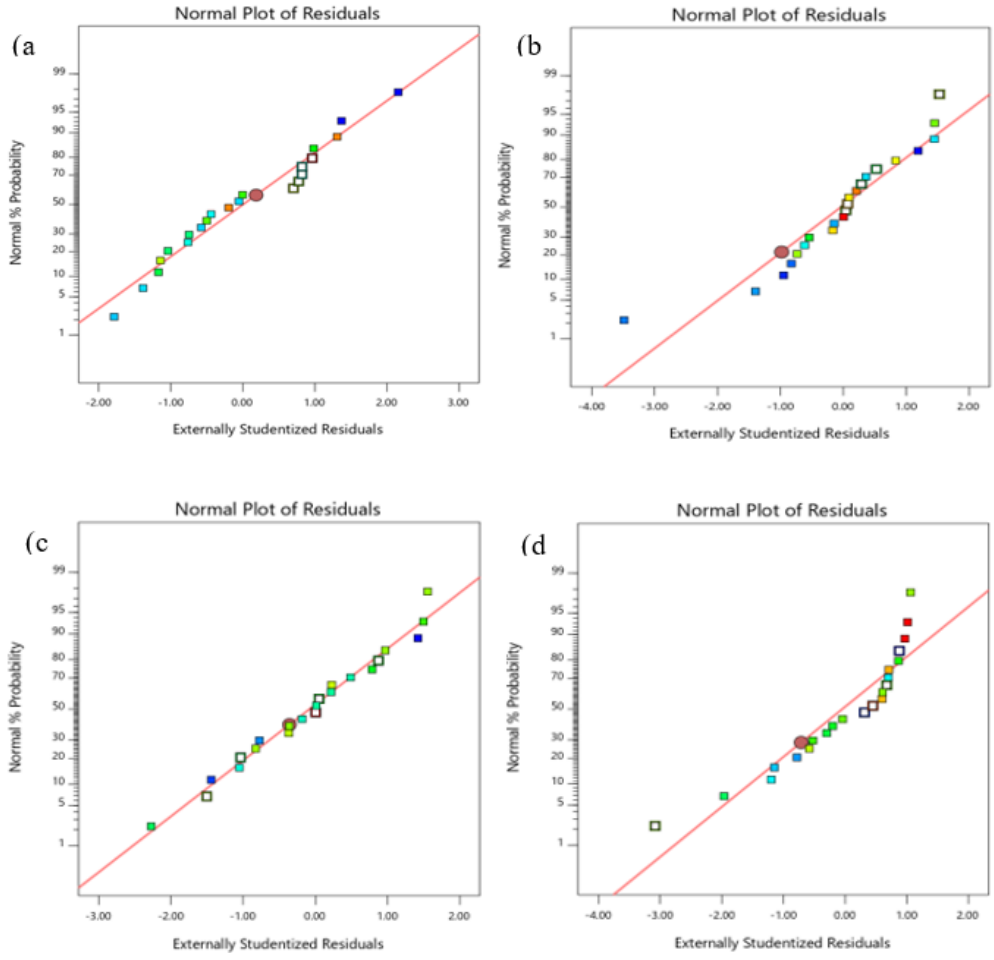

Figure 5 Normal probability plots of residuals for the (a) PM2.5, (b) PM10, (c) UFP, and (d) TSP response surface models.

3.3. Interaction effects of Factor A and B in PM2.5, PM10, UFP and TSP

Figure 6 (a) shows the contour plot of the interaction effects between Factors A (refresh rate) and B (collecting powder from the mixing machine) on the PM2.5, and Figure 6(b) shows the corresponding 3D response surface plot. It can be observed that the PM2.5 decreases as Factors A and B increase. This indicates that the PM2.5 decreases when higher amounts of recycled powder are used and the powder is half-covered when it is collected from the mixing machine. This finding is aligned with the results of Clayton and Deffley (2014), who found that particle size distribution had shifted slightly to larger diameters during the sintering process. Oxidation, which occurs during the sintering process, may influence the particle size distribution of the PA12 powder, which explains why the PM2.5 is reduced after the sintering process. Equation (4) represents the regression model for PM2.5 and it indicates the variability of PM2.5 as a function of Factors A, B, and C.

$$\text{PM2.5} = 0.4361 - 0.1730A - 0.0008B + 0.0227C - 0.0074AB - 0.0257AC - 0.0465BC + 0.2176B^2 \quad (4)$$

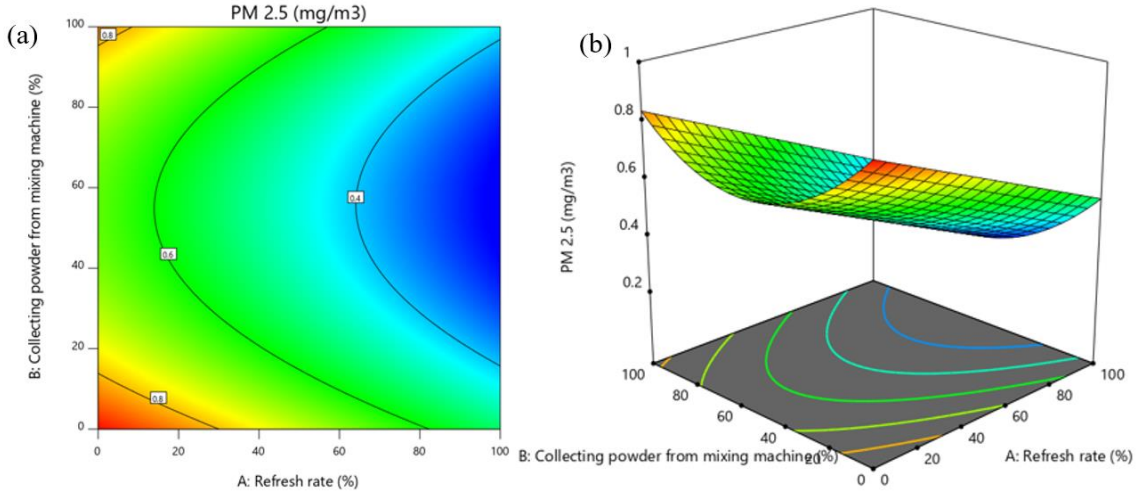

Figure 6. Interaction effects of Factors A (refresh rate) and B (collecting the powder from the mixing machine) on the PM 2.5: (a) contour plot and (b) 3D response surface plot.

Figure 7(a) and (b) show the contour plot and corresponding 3D response surface plot for PM10. It can be observed that the PM10 can be reduced to 0.4 mg/m^3 by partially covering the powder when collecting the powder from the mixing machine (Factor B) and setting the refresh rate (Factor A) as follows: 60% virgin powder + 40% recycled powder. The PM10 is minimum at a refresh rate of 100%, which indicates the full use of recycled powder during the pre-processing activities of the SLS 3D printing process. Based on the results, collecting virgin powder from the mixing machine will release higher amounts of PM10 compared with collecting recycled powder. This finding contradicts the results of Graff et al. (2017), who discovered that the particle size of recycled powder was smaller than that of virgin powder. The particle size distribution is within a range of 40–80 µm, which is larger than 10 µm (PM10). Equation (5) represents the variability of PM10 as a function of Factors A, B, and C.

$$\text{PM10} = 0.4768 - 0.0959A - 0.0258B + 0.0504C - 0.0716AB - 0.0484A^2 + 0.2081B^2 \quad (5)$$

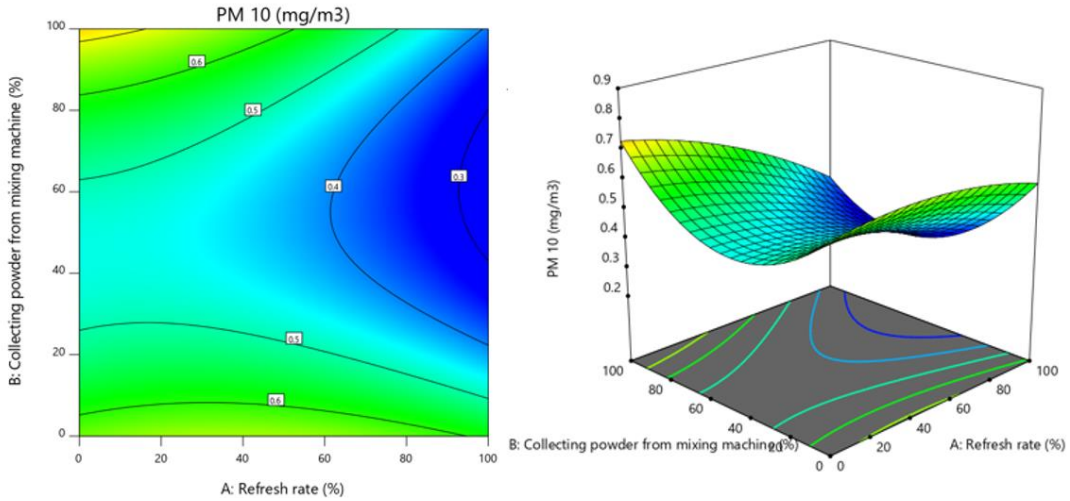

Figure 7. Interaction effects of Factors A (refresh rate) and B (collecting the powder from the mixing machine) on the PM10: (a) contour plot and (b) 3D response surface plot.

Figures 8 (a) and (b) show the contour plot and corresponding 3D response surface plot for UFP. It can be observed that the UFP is minimized (5000 pt/cc) when Factor A (refresh rate) is roughly 90% and Factor B (collecting the powder from the mixing machine) is 50%, which means that the powder is half-covered during this pre-processing activity. It can be observed that the UFP is minimized when recycled. It is evident from the results that the UFP is significantly influenced by the use of virgin powder and thus, it is crucial to ensure proper handling of the virgin powder with the appropriate personal protective equipment of virgin powder during the pre-processing activities of the SLS 3D printing process. The use of virgin powder will promote the particle size distribution for UFP whereas the use of recycled powder will reduce the particle size distribution of UFP (Arrizubieta et al., 2020). Equation (6) represents the regression model for UFP as a function of Factors A, B, and C.

$$UFP = 5455.63 - 296.42A + 8.83B + 98.2C + 111.13AB + 66.08AC - 14BC - 15.33A^2 + 199.92B^2 + 87.62ABC + 83.22A^2C \quad (6)$$

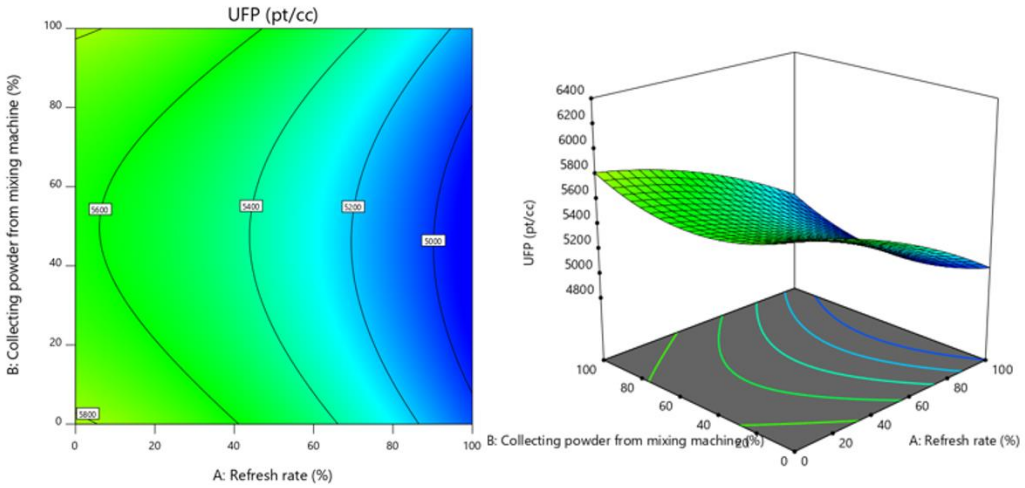

Figure 8 Interaction effects of Factors A (refresh rate) and B (collecting the powder from the mixing machine) on the UFP: (a) contour plot and (b) 3D response surface plot.

Figure 9 (a) and (b) show the contour plot and 3D response surface plot for TSP. It can be seen that the TSP is minimized when Factor A (refresh rate) is 50% (i.e., 50% virgin powder + 50% recycled powder), which differs from that for other response variables (PM2.5, PM10, and UFP). The particle size distribution of the PA12 powder is within a range of 40–80 µm. The TSP was measured based on the size of the emitted dust unlike the other parameters (PM2.5, PM10, and UFP). The TSP is high when the Factor A (refresh rate) is 50% and Factor B (collecting the powder from mixing machine) is 60%. In other words, the TSP is high even when the powder is partially covered (60%) when it is collected from the mixing machine. The results suggest that most of the particles dispersed in the SLS Laboratory are fine powders. The TSP indicates that the mean particle size is distributed somewhat within PM2.5 and PM10, which are the key factors to the dustiness (Lilao et al., 2017). Equation (7) represents the variability of the TSP as a function of Factors A, B, and C.

$$TSP = 0.4086 + 0.0085A + 0.0087B + 0.0062C - 0.0094AB + 0.0068AC - 0.0044BC - 0.0138A^2 - 0.0320B^2 \quad (7)$$

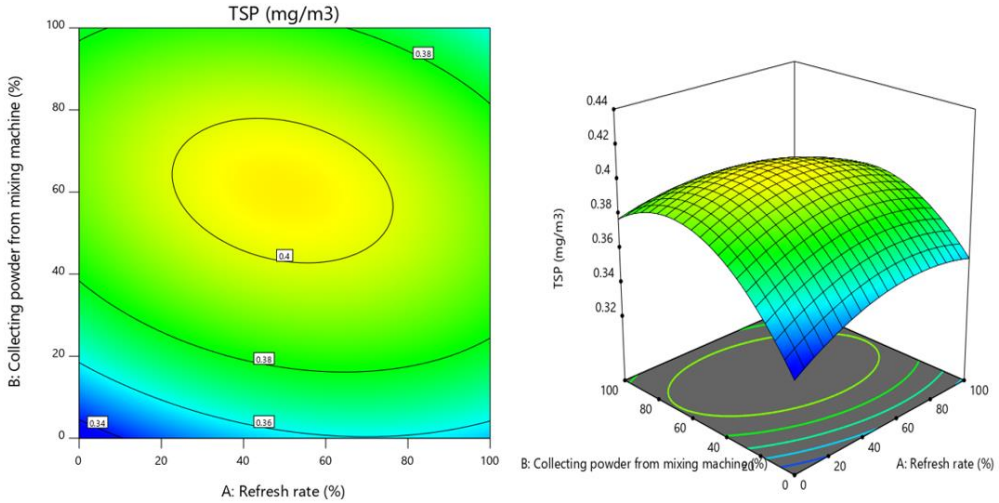

Figure 9 Interaction effects of Factors A (refresh rate) and B (collecting the powder from the mixing machine) on the TSP: (a) contour plot and (b) 3D response surface plot.

3.4. Optimization of Factor A,B and C

Optimization is dependent on the desirability of the factors (input variables) and response variables, where the desirability falls within a range of 0–1. The criteria for the optimization process are as follows: (1) upper and lower limits for each parameter, (2) weight, (3) criteria, and (4) importance of the parameters, as shown in Table 4. If the importance value is the same for all response variables, the value of the objective function will be reduced to the standard conditions for desirability (Yusri et al., 2017). In this study, the main objective of the optimization is to minimize the response variables during the pre-processing activities of the SLS 3D printing process. The desirability value is highest (0.816) for the following settings: (1) Factor A: 100% (100% recycled powder), (2) Factor B: 33% (the powder is 33% when it is collected from the mixing machine: 33%), and (3) Factor C: full cover (the powder is completely covered when it is transferred to the SLS 3D printer). These are the optimal settings, which results in the highest desirability for all response variables. At these settings, the PM2.5, PM10, UFP, and TSP are found to be 0.2787 mg/m^3, 0.3404 mg/m^3, 4904 pt/cc, and 0.3852 mg/m^3, respectively, as shown in Figure 10.

Table 4 Criteria used to optimize the response variables (PM2.5, PM10, UFP, and TSP).

Parameters	Limits		Criterion	Importance
	Lower	Upper		
A. Refresh rate (%)	0	100	Within range	3
B. Collecting the powder from the mixing machine (%)	0	100	Within range	3
C. Transferring the powder to the SLS 3D printer (full cover/no cover)	Full cover	No cover	Within range	3
PM2.5 (mg/m^3)	0.273	0.920	Minimize	3
PM10 (mg/m^3)	0.336	0.829	Minimize	3
UFP (mg/m^3)	4904	6256	Minimize	3
TSP (mg/m^3)	0.338	0.424	Minimize	3

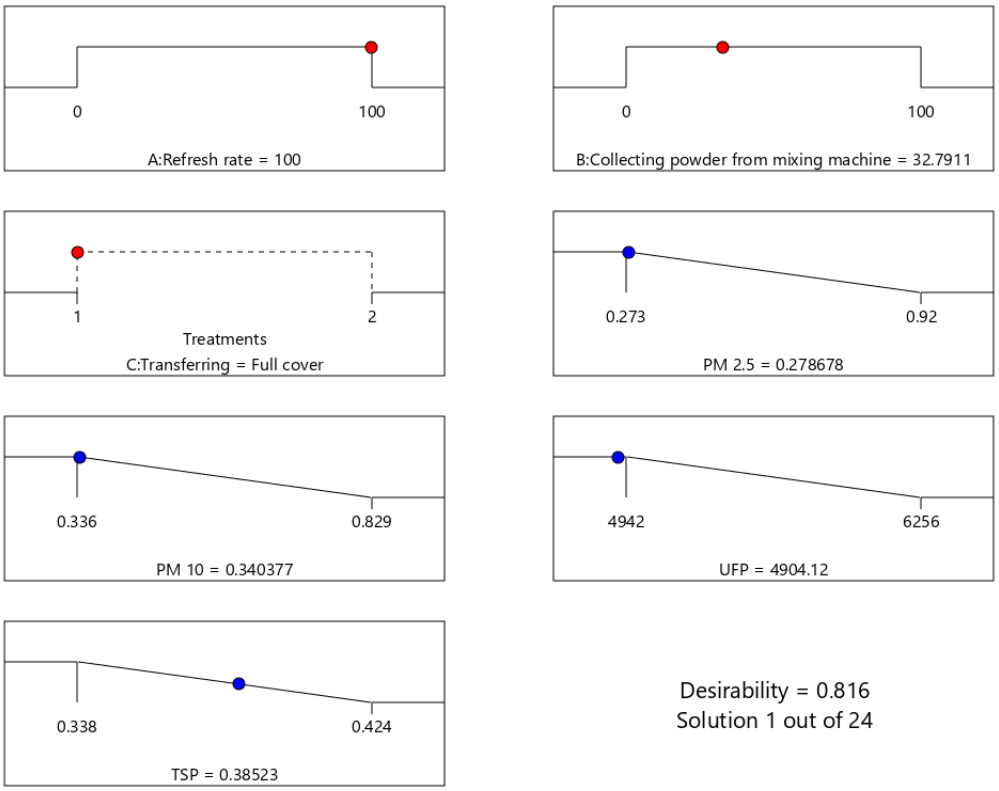

Figure 10 Optimal settings for the refresh rate and pre-processing activities that will maximize the desirability value and minimize the PM2.5, PM10, UFP, and TSP for SLS 3D printing.

3.5. Validation of the optimal settings predicted by response surface models.

To validate the results predicted by the response surface models, five experiments were performed using the predicted optimal settings: (1) Factor A: 100% (100% recycled powder), (2) Factor B: 33% (the powder is covered by 33% when it is collected from the mixing machine), and (3) Factor C: full cover (the powder is completely covered when it is transferred to the SLS 3D printer). The average PM2.5, PM10, UFP, and TSP were determined based on the data obtained from the validation

experiments. The results are summarized in Table 5, along with the predicted values and percentage difference. The percentage difference was calculated using Equation (8). In general, the percentage difference is less than 5% for the response variables (PM2.5, PM10, UFP, and TSP), indicating that there is good agreement between the predicted and experimental values (Yusri et al., 2017). The results indicate that the PM2.5, PM10, UFP, and TSP response surface models can reliably predict the PM2.5, PM10, UFP, and TSP as a function of the refresh rate and pre-processing activities considered in this study.

$$\text{Percentage difference} = \left(\frac{\text{Experimental value} - \text{Predicted value}}{\text{Exprimental value}}\right) \times 100 \qquad (8)$$

Table 5 Results of the validation experiments.

Factor A: refresh rate (%)	Factor B: Collecting the powder from the mixing machine (%)	C. Transferring the powder to the SLS 3D printer (full cover/no cover)		PM 2.5 (mg/m^3)	PM 10 (mg/m^3)	UFP (pt/cc)	TSP (mg/m^3)
100 (recycled)	33	Full cover	Predicted	0.266	0.282	4896	0.390
			Actual	0.278	0.293	5132	0.399
				±3.54	±4.20	±2.07	±1.53
			Percentage of absolute error (%)	4.33	3.57	4.56	2.38

4. Conclusion

In this study, the refresh rate and pre-processing activities were optimized using RSM in order to minimize the dust exposure in terms of the PM2.5, PM10, UFP, and TSP, where PA12 powder was chosen as the powder for SLS 3D printing. The following conclusions were drawn based on the findings:

1. Based on the ANOVA results, the PM2.5, PM10, UFP, and TSP response surface models are statistically significant, with a p-value of less than 0.0001.
2. The virgin powder (PA 12 nylon) is found to be more minute and therefore, the powder particulates are more inhalable and respirable compared with recycled powder (PA12 nylon). This contradicts the findings of Graff et al. (2017), where found that recycled metal powder for SLS 3D printing is smaller than virgin powder.
3. Based on the RSM results, the following settings can minimize the PM2.5, PM10, UFP, and TSP during the pre-processing activities of SLS 3D printing: (1) Factor A: 100% (100% recycled powder), (2) Factor B: 33% (the process is 33 percent cover when it is collected from the mixing machine), and (3) Factor C: full cover (the powder is completely covered when it is transferred to the SLS 3D printer. These optimal settings give the highest desirability value of 0.816.
4. Based on the results obtained from the validation experiments, the four response surface models are all reliable to predict the PM2.5, PM10, UFP, and TSP as a function of the refresh rate and pre-processing activities considered in this study, where the percentage difference between the predicted and experimental values is less than 5%.
5. RSM based on the central composite design can considerably reduce time and cost by minimizing the number of experiments and the response surface models are proven to be statistically significant for all response variables.
6. The development of mitigation strategies such local exhaust ventilation and dust control based on specific task of pre processing activities of powder handling is suggested for future works.

Acknowledgment

The authors graciously thank the Faculty of Mechanical Technology and Engineering (FTKM), Universiti Teknikal Malaysia Melaka (UTeM), for providing the materials, instruments, equipment, and facilities used in this study.

Ethical considerations

Not applicable.

Conflict of Interest

The authors declare that they have no known competing financial interests or personal relationships that could have appeared to influence the work reported in this paper.

Funding

This research did not receive any financial support.

References

Abdalla, A.N., Tao, H., Bagaber, S.A., Ali, O.M., Kamil, M., Ma, X., Awad, O.I., 2019. Prediction of emissions and performance of a gasoline engine running with fusel oil–gasoline blends using response surface methodology. Fuel 253, 1–14. https://doi.org/10.1016/j.fuel.2019.04.085

Afshar-Mohajer, N., Wu, C.Y., Ladun, T., Rajon, D.A., Huang, Y., 2015. Characterization of particulate matters and total VOC emissions from a binder jetting 3D printer. Build. Environ. 93, 293–301. https://doi.org/10.1016/j.buildenv.2015.07.013

Ansart, R., Letourneau, J.J., de Ryck, A., Dodds, J.A., 2011. Dust emission by powder handling: Influence of the hopper outlet on the dust plume. Powder Technol. 212, 418–424. https://doi.org/10.1016/j.powtec.2011.06.022

Arrizubieta, J.I., Ukar, O., Ostolaza, M., Mugica, A., 2020. Study of the environmental implications of using metal powder in additive manufacturing and its handling. Metals (Basel). 10. https://doi.org/10.3390/met10020261

Baby, A., Alexander, A.A., 2018. A Review on Various Techniques used in Predicting Pollutants. IOP Conf. Ser. Mater. Sci. Eng. 396. https://doi.org/10.1088/1757-899X/396/1/012016

Bezerra, M.A., Santelli, R.E., Oliveira, E.P., Villar, L.S., Escaleira, L.A., 2008. Response surface methodology (RSM) as a tool for optimization in analytical chemistry. Talanta 76, 965–977. https://doi.org/10.1016/j.talanta.2008.05.019

Bours, J., Adzima, B., Gladwin, S., Cabral, J., Mau, S., 2017. Addressing Hazardous Implications of Additive Manufacturing: Complementing Life Cycle Assessment with a Framework for Evaluating Direct Human Health and Environmental Impacts. J. Ind. Ecol. 21, S25–S36. https://doi.org/10.1111/jiec.12587

Butler, J., 2011. Using selective laser sintering for manufacturing. Assem. Autom. 31, 212–219. https://doi.org/10.1108/01445151111150541

Chan, F.L., House, R., Kudla, I., Lipszyc, J.C., Rajaram, N., Tarlo, S.M., 2018. Health survey of employees regularly using 3D printers. Occup. Med. (Chic. Ill). 68, 211–214. https://doi.org/10.1093/occmed/kqy042

Chen, P., Wu, H., Zhu, W., Yang, L., Li, Z., Yan, C., Wen, S., Shi, Y., 2018. Investigation into the processability, recyclability and crystalline structure of selective laser sintered Polyamide 6 in comparison with Polyamide 12. Polym. Test. 69, 366–374. https://doi.org/10.1016/j.polymertesting.2018.05.045

Clayton, J., Deffley, R., 2014. Optimising metal powders for additive manufacturing. Met. Powder Rep. 69, 14–17. https://doi.org/10.1016/S0026-0657(14)70223-1

Copelli, S., Barozzi, M., Scotton, M.S., Fumagalli, A., Derudi, M., Rota, R., 2019. A predictive model for the estimation of the deflagration index of organic dusts. Process Saf. Environ. Prot. 126, 329–338. https://doi.org/10.1016/j.psep.2019.04.012

Dadbakhsh, S., Verbelen, L., Vandeputte, T., Strobbe, D., Van Puyvelde, P., Kruth, J.P., 2016. Effect of powder size and shape on the SLS processability and mechanical properties of a TPU elastomer. Phys. Procedia 83, 971–980. https://doi.org/10.1016/j.phpro.2016.08.102

Dadbakhsh, S., Verbelen, L., Verkinderen, O., Strobbe, D., Van Puyvelde, P., Kruth, J.P., 2017. Effect of PA12 powder reuse on coalescence behaviour and microstructure of SLS parts. Eur. Polym. J. 92, 250–262. https://doi.org/10.1016/j.eurpolymj.2017.05.014

Damanhuri, Amir Abdullah Muhamad, Azian Hariri, Alkahari, M.R., Fauadi, M.H.F., Bakri, S.F.Z., 2019. Indoor air concentration from selective laser sintering 3D printer using virgin polyamide nylon (PA12) powder: A pilot study. Int. J. Integr. Eng. 11, 140–149. https://doi.org/10.30880/ijie.2019.11.05.019

Damanhuri, A. A.M., Subki, A.S.A., Hariri, A., Tee, B.T., Fauadi, M.H.F.M., Hussin, M.S.F., Mustafa, M.S.S., 2019. Comparative study of selected indoor concentration from selective laser sintering process using virgin and recycled polyamide nylon (PA12), in: IOP Conference Series: Earth and Environmental Science. https://doi.org/10.1088/1755-1315/373/1/012014

Dimov, S.S., Pham, D.T., Lacan, F., Dotchev, K.D., 2001. Rapid tooling applications of the selective laser sintering process. Assem. Autom. 21, 296–302. https://doi.org/10.1108/EUM0000000006011

DOSH Malaysia, 2010. Industry Code of Practice on Indoor Air Quality 2010, JKKP DP (S) 127/379/4-39. Minist. Hum. Resour. Dep. Occup. Saf. Heal. 1–50. https://doi.org/http://dx.doi.org/10.1016/0965-8564(95)90299-6

Dotchev, K., Yusoff, W., 2009. Recycling of polyamide 12 based powders in the laser sintering process. Rapid Prototyp. J. 15, 192–203. https://doi.org/10.1108/13552540910960299

Du Preez, S., Johnson, A., LeBouf, R.F., Linde, S.J.L., Stefaniak, A.B., Du Plessis, J., 2018a. Exposures during industrial 3-D printing and post-processing tasks. Rapid Prototyp. J. 24, 865–871. https://doi.org/10.1108/RPJ-03-2017-0050

Du Preez, S., Johnson, A., LeBouf, R.F., Linde, S.J.L., Stefaniak, A.B., Du Plessis, J., 2018b. Exposures during industrial 3-D printing and post-processing tasks. Rapid Prototyp. J. 24, 865–871. https://doi.org/10.1108/RPJ-03-2017-0050

Eyers, D.R., Potter, A.T., 2017. Industrial Additive Manufacturing: A manufacturing systems perspective. Comput. Ind. 92–93, 208–218. https://doi.org/10.1016/j.compind.2017.08.002

Farsoon Technologies, 2018. Metal & Polymer Materials for Additve Manufacturing.

Ford, S., Despeisse, M., 2016. Additive manufacturing and sustainability: an exploratory study of the advantages and challenges. J. Clean. Prod. 137, 1573–1587. https://doi.org/10.1016/j.jclepro.2016.04.150

Ghani, S.A., Muhamad, N.A., Noorden, Z.A., Zainuddin, H., Ahmad, A.A., 2017. Multi-response optimization of the properties of natural ester oil with mixed antioxidants using taguchi-based methodology. IEEE Trans. Dielectr. Electr. Insul. 24, 1674–1684. https://doi.org/10.1109/TDEI.2017.006589

Gopal, K., Sathiyagnanam, A.P., Rajesh Kumar, B., Saravanan, S., Rana, D., Sethuramasamyraja, B., 2018. Prediction of emissions and performance of a diesel engine fueled with n-octanol/diesel blends using response surface methodology. J. Clean. Prod. 184, 423–439. https://doi.org/10.1016/j.jclepro.2018.02.204

Graff, P., Ståhlbom, B., Nordenberg, E., Graichen, A., Johansson, P., Karlsson, H., 2017a. Evaluating Measuring Techniques for Occupational Exposure during Additive Manufacturing of Metals: A Pilot Study. J. Ind. Ecol. 21, S120–S129. https://doi.org/10.1111/jiec.12498

Graff, P., Ståhlbom, B., Nordenberg, E., Graichen, A., Johansson, P., Karlsson, H., 2017b. Evaluating Measuring Techniques for Occupational Exposure during Additive Manufacturing of Metals: A Pilot Study. J. Ind. Ecol. 21, 120–129. https://doi.org/10.1111/jiec.12498

House, R., Rajaram, N., Tarlo, S.M., 2017. Case report of asthma associated with 3D printing. Occup. Med. (Chic. Ill). 67, 652–654. https://doi.org/10.1093/occmed/kqx129

Huang, Y., Leu, M.C., Mazumder, J., Donmez, A., 2015. Additive Manufacturing: Current State, Future Potential, Gaps and Needs, and Recommendations. J. Manuf. Sci. Eng. 137, 014001. https://doi.org/10.1115/1.4028725

Ismail, A.R., Rani, M.R.A., Md. Deros, B., Makhbul, Z.K.M., Mohd Yusof, M.Y., 2012. Response Surface Method in Modelling the Environmental Factors Toward Workers' Productivity. J. Occup. Saf. Heal. 9, 83–90.

Kellens, K., Renaldi, R., Dewulf, W., Kruth, J.P., Duflou, J.R., 2014. Environmental impact modeling of selective laser sintering processes. Rapid Prototyp. J. 20, 459–470. https://doi.org/10.1108/RPJ-02-2013-0018

Khoobbakht, G., Najafi, G., Karimi, M., Akram, A., 2016. Optimization of operating factors and blended levels of diesel, biodiesel and ethanol fuels to minimize

exhaust emissions of diesel engine using response surface methodology. Appl. Therm. Eng. 99, 1006–1017. https://doi.org/10.1016/j.applthermaleng.2015.12.143

Kolb, T., Kolb, T., Schmidt, P., Beisser, R., Tremel, J., Schmidt, M., 2017. Safety in additive manufacturing: Fine dust measurements for a process chain in Laser beam melting of metals. RTeJournal - Fachforum für Rapid Technol. 2017.

Koponen, I.K., Koivisto, A.J., Jensen, K.A., 2015. Worker exposure and high time-resolution analyses of process-related submicrometre particle concentrations at mixing stations in two paint factories. Ann. Occup. Hyg. 59, 749–763. https://doi.org/10.1093/annhyg/mev014

Lilao, A.L., Forner, V.S., Gasch, G.M., Gimeno, E.M., 2017. Particle size distribution: A key factor in estimating powder dustiness. J. Occup. Environ. Hyg. 14, 975–985. https://doi.org/10.1080/15459624.2017.1358818

Ljunggren, S.A., Karlsson, H., Ståhlbom, B., Krapi, B., Fornander, L., Karlsson, L.E., Bergström, B., Nordenberg, E., Ervik, T.K., Graff, P., 2019a. Biomonitoring of

N. Afshar-Mohajer, C. Y. Wu, T. Ladun, D. A. Rajon, and Y. Huang, "Characterization of particulate matters and total VOC emissions from a binder jetting 3D printer," Build. Environ., vol. 93, no. P2, pp. 293–301, 2015.

Metal Exposure During Additive Manufacturing (3D Printing). Saf. Health Work 10, 518–526. https://doi.org/10.1016/j.shaw.2019.07.006

Ljunggren, S.A., Karlsson, H., Ståhlbom, B., Krapi, B., Fornander, L., Karlsson, L.E., Bergström, B., Nordenberg, E., Ervik, T.K., Graff, P., 2019b. Biomonitoring of Metal Exposure During Additive Manufacturing (3D Printing). Saf. Health Work. https://doi.org/10.1016/j.shaw.2019.07.006

Montgomery, D.C., 2017. Design and Analysis of Experiments, 9th Edition, Hoboken, Wiley.

Ngo, T.D., Kashani, A., Imbalzano, G., Nguyen, K.T.Q., Hui, D., 2018. Additive manufacturing (3D printing): A review of materials, methods, applications and challenges. Compos. Part B Eng. 143, 172–196. https://doi.org/10.1016/j.compositesb.2018.02.012

Norhan, S.N., Zainuddin, H., Ghani, S.A., Chairul, I.S., 2017. Optimization of the mixing process parameters to enhance the dielectric strength of mineral and palm fatty acid ester insulating oil blends. J. Electr. Syst. 13, 595–605.

Plinke, M.A.E., Leith, D., Boundy, M.G., Löffler, F., 1995. Dust generation from handling powders in industry. Am. Ind. Hyg. Assoc. J. 56, 251–257. https://doi.org/10.1080/15428119591017088

Prakash, K.S., Nancharaih, T., Rao, V.V.S., 2018. Additive Manufacturing Techniques in Manufacturing -An Overview, in: Materials Today: Proceedings. pp. 3873–3882. https://doi.org/10.1016/j.matpr.2017.11.642

Preez, S. Du, Johnson, A., Lebouf, R.F., Linde, S.J.L., Stefaniak, A.B., Plessis, J. Du, Preez, S. Du, Johnson, A., Lebouf, R.F., Linde, S.J.L., Stefaniak, A.B., Plessis, J. Du, Preez, S. Du, Johnson, A., Lebouf, R.F., Plessis, J. Du, 2018. Exposures during industrial 3-D printing and post-processing tasks. https://doi.org/10.1108/RPJ-03-2017-0050

Rejeski, D., Zhao, F., Huang, Y., 2018. Research needs and recommendations on environmental implications of additive manufacturing. Addit. Manuf. 19, 21–28. https://doi.org/10.1016/j.addma.2017.10.019

Short, D.B., Sirinterlikci, A., Badger, P., Artieri, B., 2015. Environmental, health, and safety issues in rapid prototyping. Rapid Prototyp. J. 21, 105–110. https://doi.org/10.1108/RPJ-11-2012-0111

Silva, A.F., Neves, P., Rocha, S.M., Silva, C.M., Valente, A.A., 2020. Optimization of continuous-flow heterogeneous catalytic oligomerization of 1-butene by design of experiments and response surface methodology. Fuel 259, 116256. https://doi.org/10.1016/j.fuel.2019.116256

Stefaniak, A.., Johnson, A.., Preez, S. d., Hammond, D.., Wells, J.R., Ham, J.E., LeBouf, R.., Jr, S.. M., Duling, M.., Bowers, L.., Knepp, A.., Beer, D.. de, Plessis, J.. du, 2018. Insights Into Emissions and Exposures From Use of Industrial Scale Additive Manufacturing Machines. Saf. Heal 8, 1–8.

Tiwari, S.K., Pande, S., Agrawal, S., Bobade, S.M., 2015. Selection of selective laser sintering materials for different applications. Rapid Prototyp. J. 21, 630–648. https://doi.org/10.1108/RPJ-03-2013-0027

Väisänen, A.J.K., Hyttinen, M., Ylönen, S., Alonen, L., 2018. Occupational exposure to gaseous and particulate contaminants originating from additive manufacturing of liquid, powdered, and filament plastic materials and related post-processes. J. Occup. Environ. Hyg. 16, 258–271. https://doi.org/10.1080/15459624.2018.1557784

Way, Y., Pham, D.T., Dotchev, K.D., 2014. Investigation of the Thermal Properties of Different Grades Polyamide 12 (PA12) in Improving Laser Sintering Process (SLS). Appl. Mech. Mater. 548–549, 294–296. https://doi.org/10.4028/www.scientific.net/amm.548-549.294

Wong, K. V., Hernandez, A., 2012. A Review of Additive Manufacturing. ISRN Mech. Eng. 2012, 1–10. https://doi.org/10.5402/2012/208760

Wypych, P., Cook, D., Cooper, P., 2005. Controlling dust emissions and explosion hazards in powder handling plants. Chem. Eng. Process. Process Intensif. 44, 323–326. https://doi.org/10.1016/j.cep.2004.02.026

Yusri, I.M., Mamat, R., Azmi, W.H., Omar, A.I., Obed, M.A., Shaiful, A.I.M., 2017. Application of response surface methodology in optimization of performance and exhaust emissions of secondary butyl alcohol-gasoline blends in SI engine. Energy Convers. Manag. 133, 178–195. https://doi.org/10.1016/j.enconman.2016.12.001

Zarringhalam, H., Hopkinson, N., Kamperman, N.F., Vlieger, J.J. De, 2006. Effects of processing on microstructure and properties of SLS Nylon 12 436, 172–180. https://doi.org/10.1016/j.msea.2006.07.084

Zisook, R.E., Simmons, B.D., Vater, M., Perez, A., Ellen, P., Paustenbach, D.J., Cyrs, W.D., Zisook, R.E., Simmons, B.D., Vater, M., Perez, A., Ellen, P., Paustenbach, D.J., Cyrs, W.D., 2020. Emissions associated with operations of four different additive manufacturing or 3D printing technologies. J. Occup. Environ. Hyg. 0, 1–16. https://doi.org/10.1080/15459624.2020.1798012

Zontek, T.L., Ogle, B.R., Jankovic, J.T., Hollenbeck, S.M., 2017. An exposure assessment of desktop 3D printing. J. Chem. Heal. Saf. 24, 15–25. https://doi.org/10.1016/j.jchas.2016.05.008